REPORT DOCUMENTATION PAGE

AFRL-SR-AR-TR-02-

0289

1. REPORT DATE (DD-MM-YYYY)	2. REPORT TYPE	3. DATES COVERED (From - To)
08/10/2002	Final Performance Report	05/15/1998 - 05/15/2002

4. TITLE AND SUBTITLE
Textures in Aluminum and Titanium: Their On-Line Evaluation and Quantitative Effects on Formability

5a. CONTRACT NUMBER
F49620-98-1-0469

5b. GRANT NUMBER

5c. PROGRAM ELEMENT NUMBER

6. AUTHOR(S)
Chi-Sing Man

5d. PROJECT NUMBER

5e. TASK NUMBER

5f. WORK UNIT NUMBER

7. PERFORMING ORGANIZATION NAME(S) AND ADDRESS(ES)

University of Kentucky
Research Foundation
201 Kinkead Hall
Lexington, KY 40506-0057

8. PERFORMING ORGANIZATION REPORT NUMBER

20020909 128

9. SPONSORING / MONITORING AGENCY NAME(S) AND ADDRESS(ES)
USAF, AFRL
Air Force Office of
Scientific Research
801 N Randolph St., Room 732
Arlington, VA 22203

10. SPONSOR/MONITOR'S ACRONYM(S)
AFOSR/NM

11. SPONSOR/MONITOR'S REPORT NUMBER(S)

12. DISTRIBUTION / AVAILABILITY STATEMENT
Approved for public release; distribution is unlimited.

13. SUPPLEMENTARY NOTES

14. ABSTRACT
The main findings of this project were as follows: (1) For samples of an AA5xxx aluminum alloy sheet at temperatures up to 750°F, the degree of recrystallization could be monitored by using either resonance-EMAT spectroscopy or laser-ultrasound resonance spectroscopy. (2) Formulae showing explicitly the effects of crystallographic texture on the planar plastic anisotropy of sheets of cubic (e.g., aluminum) and of hexagonal (e.g., titanium) metals in uniaxial tension tests were derived. (3) A constitutive relation pertaining to acousto-elasticity was formulated for prestressed, orthorhombic aggregates of cubic crystallites. (4) For vertically-heterogeneous, prestressed orthorhombic media where the principal stress directions agree with the axes of orthorhombic material symmetry, a high-frequency asymptotic formula was derived which relate the depth variations of stress and texture to the dispersion of surface acoustic waves propagating in a symmetry direction.

15. SUBJECT TERMS
crystallographic texture, recrystallization in aluminum, plastic anisotropy, sheet metals, acoustoelasticity, nondestructive evaluation

16. SECURITY CLASSIFICATION OF:			17. LIMITATION OF ABSTRACT	18. NUMBER OF PAGES	19a. NAME OF RESPONSIBLE PERSON
a. REPORT	b. ABSTRACT	c. THIS PAGE		11	19b. TELEPHONE NUMBER (include area code)

FINAL PERFORMANCE REPORT
(F49620-98-1-0469. PI: Chi-Sing Man)

Excecutive Summary

The main findings of this project were as follows:

(1) For samples of an AA5xxx aluminum alloy sheet at temperatures up to 750°F, the degree of recrystallization could be monitored via measurement of the velocity ratio κ by using either resonance-EMAT spectroscopy or laser-ultrasound resonance spectroscopy, provided that the temperature of the sample in question is ascertained by another means. Both of the aforementioned ultrasound techniques have potential for on-line applications.

(2) Formulae showing explicitly the effects of crystallographic texture on the angular dependence of the q-value and of the uniaxial flow stress in sheets of cubic (e.g., aluminum) and of hexagonal (e.g., titanium) metals were derived. By isolating the effects of texture, these formulae will facilitate further studies on the influences of other microstructural factors on plastic anisotropy of sheet metals.

(3) A constitutive relation pertaining to acoustoelasticity was formulated for prestressed, orthorhombic aggregates of cubic crystallites. This constitutive relation will serve as the basis for all further work in acoustoelasticity for the class of polycrystalline materials in question.

(4) For vertically-heterogeneous, prestressed orthorhombic media where the principal stress directions agree with the axes of orthorhombic material symmetry, a high-frequency asymptotic formula was derived which relate the depth variations of stress and texture to the dispersion of surface acoustic waves propagating in a symmetry direction. Here the elastic medium in question is taken as occupying a half-space. This theory and its further developments have an important potential application in the nondestructive inspection of the thin layer of inhomogeneous stress induced by surface enhancement techniques such as shot peening, laser shock peening, and low plasticity burnishing.

Personnel Associated with this Project

- Principal investigator: Chi-Sing Man.
- Co-principal investigator: James G. Morris.
- Postdoctoral associates: Wenchang Liu, Yansheng Liu.
- Graduate students: Xiang-Ming Cheng, Mojia Huang, Jianbo Li, Leigh Noble, Roberto Paroni, Yu Xiang.
- Undergraduate students: Jamey Young.
- Others: Ying Zhang, research associate; Xingyan Fan, technician.

Publications Resulting from this Project

Journal Papers

1. C.-S. Man, "Effects of crystallographic texture on the acoustoelastic coefficients of polycrystals", *Nondestructive Testing and Evaluation*, **15**, 191--214 (1999).
2. R. Paroni and C.-S. Man, "Constitutive equations of elastic polycrystalline materials", *Arch. Rational Mech. Anal.*, **150**, 153–177 (1999).
3. Y. Liu, X.-M. Cheng, Y.L. Liu, C.-S. Man, and J.G. Morris, "Investigation of low resolution texture analyses for online R-value determination of aluminum can body materials", *Aluminum Transactions*, **2**, 311–318 (2000).
4. R. Paroni and C.-S. Man, "Two Micromechanical models in acoustoelasticity: a comparative study", *Journal of Elasticity*, **59**, 145–173 (2000).
5. C.-S. Man and L. Noble, "Designing textured polycrystals with specific isotropic material tensors: the ODF method", *Rend. Sem. Mat. Univ. Pol. Torino*, **58**, 155–170 (2000).
6. C.-S. Man and M. Huang, "Identification of material parameters in yield functions and flow rules for weakly-textured sheets of cubic metals", *International Journal of Non-Linear Mechanics*, **36**, 501–514 (2001).
7. W.C. Liu, C.-S. Man, and J.G. Morris, "Lattice rotation of the cube orientation to the ß fiber during cold rolling of AA 5052 aluminum alloy", *Scripta Materialia*, **45**, 807–814 (2001).
8. C.-S. Man, X. Fan, J.G. Morris, and K. Kawashima, "Monitoring of primary recrystallization in aluminum alloy by resonance EMAT spectroscopy", *Materials Science Forum*, in press.
9. C.-S. Man, "On the *r*-value of textured sheet metals", *Int. J. Plasticity*, in press.

Papers in Conference Proceedings

1. C.-S. Man, "Material tensors of weakly-textured polycrystals", in *Proceedings of the Third International Conference on Nonlinear Mechanics (ICNM-III)*, Chien Wei-zang et al. (eds.), Shanghai University Press, Shanghai, 1998, pp. 87–94.
2. J. Li, and C.-S. Man, "Free Rayleigh waves in anisotropic half-space coated with prestressed thin film", in Proceedings of the Third International Conference on Nonlinear Mechanics (ICNM-III), Chien Wei-zang et al. (eds.), Shanghai University Press, Shanghai, 1998, pp. 277–281.
3. C.-S. Man, "Effects of texture on plastic anisotropy in sheet metals", in *Nondestructive Characterization of Materials VIII*, R.E. Green, Jr. (ed.), Plenum Press, New York, 1998, pp. 751–756.
4. C.-S. Man and J.D. Young, "A quadratic plastic potential for weakly-textured orthorhombic sheets of hexagonal metals", in *Applied Mechanics in the Americas*, Vol. 7, P.B. Goncalves et al. (eds.), American Academy of Mechanics, Philadelphia, 1999, pp. 875–878.
5. C.-S. Man, W.-Y. Lu, and J. Li, "Effects of crystallographic texture on the acoustoelastic coefficients for Rayleigh waves in aluminum", in Review of

Progress in Quantitative Nondestructive Evaluation}, Vol. 18, D.O. Thompson and D.E. Chimenti (eds.), Plenum Press, New York, 1999, pp. 1879–1886.
6. Y. Liu, X.-M. Cheng, J.G. Morris, C.-S. Man, and M. Huang, "Textures in strip-cast AA3105 alloy and their ultrasonic characterization", in *Proceedings of the Twelfth International Conference on Textures of Materials*, Vol. 1, J.A. Szpunar (ed.), NRC Research Press, Ottawa, Canada, 1999, pp. 481–486.
7. C.-S. Man, J.G. Morris, and Y. Liu, "On-line ultrasonic monitoring of textures in aluminum alloys", in *Nondestructive Characterization of Materials IX*, R.E. Green, Jr. (ed.), American Institute of Physics, Melville, New York, 1999, pp. 425–430.
8. C.-S. Man, J. Li, W.-Y. Lu, and X. Fan, "Ultrasonic measurement of through-thickness stress gradients in textured sheet metals", *Review of Progress in Quantitative Nondestructive Evaluation*, Vol. 19, D.O. Thompson and D.E. Chimenti (eds.), American Institute of Physics, Melville, New York, 2000, pp. 1613–1620.
9. C.-S. Man, J.G. Morris, D.K. Rehbein, R.B. Thompson, Y. Liu, and X. Fan, "Ultrasonic measurement of texture coefficient W_{400} in aluminum alloys", in *Review of Progress in Quantitative Nondestructive Evaluation*, Vol. 19, D.O. Thompson and D.E. Chimenti (eds.), American Institute of Physics, Melville, New York, 2000, pp. 1645–1652.
10. C.-S. Man, X. Fan, J.G. Morris, and K. Kawashima, "Measurement of texture coefficient W_{400} of aluminum alloys by resonance EMATs", in *Nondestructive Characterization of Materials X*, R.E. Green, Jr., et al. (eds.), Elsevier Science, Oxford, 2001, pp. 395–402.
11. K. Kawashima, C.-S. Man, and M. Huang, "Measurement of acoustoelastic constants of titanium sheet by resonance EMATs", in *Review of Progress in Quantitative Nondestructive Evaluation*, Vol. 20, D.O. Thompson and D.E. Chimenti (eds.), American Institute of Physics, Melville, New York, 2001, pp. 1459–1466.
12. C.-S. Man, Y. Zhang, and Y. Xiang, "Effects of crystallographic texture on plastic anisotropy of aluminum and titanium sheets", in *Plasticity, Damage and Fracture at Macro, Micro and Nano Scales*, A.S. Khan and O. Lopez-Pamies (eds.), Neat Press, Fulton, Maryland, 2002, pp. 252–254.
13. C.-S. Man, L. Koo, and M.J. Shepard, "Dispersion of Rayleigh waves in titanium alloy resulting from inhomogeneous residual stress induced by low plasticity burnishing", *Review of Progress in Quantitative Nondestructive Evaluation*, Vol. 21, D.O. Thompson and D.E. Chimenti (eds.), American Institute of Physics, Melville, New York, 2002, pp. 1651–1658.

Final Performance Report

On-Line Monitoring of Recrystallization Texture in Aluminum Alloy

Suitable annealing, which induces recrystallization of deformed grains (primary recrystallization), improves the formability of aluminum sheets. Annealing at excessively high temperatures, however, promotes exaggerated grain growth (secondary recrystallization), which degrades formability and is undesirable.

In our studies we have accumulated strong evidence that the degree of primary recrystallization, grain growth, and secondary recrystallization of a strip-cast AA5xxx alloy sheet can be monitored, at least under laboratory conditions and at temperatures up to 750°F, by either resonance-EMAT (electromagnetic acoustic transducer) or laser-ultrasound measurements of the velocity ratio κ, provided that the temperature of the sample in question is ascertained by another means. By definition the velocity ratio

$$\kappa = \frac{V_L}{\overline{V_S}}, \tag{1}$$

where V_L is the velocity of longitudinal wave propagating through the thickness of the sheet and $\overline{V_S}$ is the average of the two through-thickness shear-wave velocities.

Supported by results of Olsen cup and earing tests, we demonstrated that different annealing history did affect the formability of AA5xxx sheets differently. We singled out the texture coefficient W_{400} as a good indicator for the degree of recrystallization and grain growth in the annealing of this AA5xxx alloy.

Theoretically we derived the formula

$$\kappa = a(T) + b(T) W_{400}, \tag{2}$$

where $a(T)$ and $b(T)$ are functions of the temperature T. Formula (2) was corroborated over a broad range of temperatures (unequivocally from room temperature to 600°F, and likely also for the range from 600°F to 750°F) in laboratory measurements on AA5xxx samples, where κ was obtained from X-ray pole figures and κ was determined both by resonance EMAT spectroscopy and by laser-ultrasound resonance spectroscopy. Hence we may monitor the degree of recrystallization by ultrasonic measurement of κ if the temperature of the sample in question is ascertained by another means. Real-time measurements of κ at 600°F, 650°F, and 700°F, coupled with the κ versus temperature plots in our data, provide convincing proof which validates the preceding assertion. More details about the resonance-EMAT measurements were reported in journal paper [8] listed in the Executive Summary.

Independently supported by a grant from the U.S. Department of Energy, plant trials on using laser-ultrasound spectroscopy for on-line monitoring of recrystallographic texture in strip-cast aluminum alloys were conducted at the Carson Rolling Mill of Commonwealth Aluminum Corporation on May 1-3, 2002. Analysis and evaluation of data obtained on-line are still in progress.

Effect of Texture on Plastic Anisotropy of Sheet Metals

Sheet metals usually exhibit anisotropic behavior in plastic flow. Uniaxial tension tests, because of their economy and convenience, are commonly used by industry for the characterization of plastic anisotropy of sheet metals. Among the microstructural factors that give rise to plastic anisotropy, crystallographic texture, as described quantitatively by the orientation distribution function (ODF) w, is perhaps the most important. In our work we consider textured sheet metals with plastic potential and yield function of the form $f(\sigma, w)$ and $g(\sigma, w)$, respectively, where σ denotes the deviator of the Cauchy stress, w is the ODF that describes the current texture, and the possible influences of other microstructural elements on f and g are left implicit. For orthorhombic sheets of cubic (e.g., aluminum) and hexagonal (e.g., titanium) metals, we derive general formulae relating the angular dependence of the r-value and of the uniaxial flow stress σ to w, which are valid up to terms linear in the texture coefficients W_{lmn}. By isolating the effects of crystallographic texture, these formulae will also facilitate further studies of the influences of other microstructural factors on plastic anisotropy.

PRELIMINARIES

We consider sheet metals, which are polycrystalline aggregates of tiny crystallites, and we restrict our discussion to the case where all the crystallites are of the same chemical composition. We choose and fix a Cartesian coordinate system in space. To describe the orientation of a crystallite, we pick as reference the configuration of a single crystal. The orientation of a crystallite in the polycrystalline aggregate is then specified by the set of rotations $\boldsymbol{R}$ which take the reference configuration to the given configuration of the crystallite. The number of elements in each set that defines an orientation is determined by the crystal symmetry of the crystallites in question.

Let G be the rotation group and G_{cr} the group of crystal symmetry. The crystallographic texture of a polycrystalline aggregate is defined by the orientation distribution function (ODF) w defined on the rotation group. For each rotation $\boldsymbol{Q}$ in G_{cr}, we have $w(\boldsymbol{RQ}) = w(\boldsymbol{R})$ for each rotation $\boldsymbol{R}$ in G. In this paper we assume that w is independent of the sampling location.

Let $\boldsymbol{e}_1$, $\boldsymbol{e}_2$, and $\boldsymbol{e}_3$ be the orthonormal basis vectors associated with the chosen coordinate system. We parametrize the rotation group G with the Euler angles (ψ, θ, ϕ). Let $L^2(G)$ be the space of square-integrable complex-valued functions on G. For $w \in L^2(G)$, we can expand it as an infinite series in terms of the Wigner D-functions:

$$w(\boldsymbol{R}) = \frac{1}{8\pi^2} + \sum_{l=1}^{\infty} \sum_{m=-l}^{l} \sum_{n=-l}^{l} c_{mn}^{l} D_{mn}^{l}(\boldsymbol{R}(\psi, \theta, \phi)),\ c_{mn}^{l} = (-1)^{m-n} \left(c_{\overline{mn}}^{l}\right)^{*}$$

where c_{mn}^{l} $(l \geq 1)$ are the texture coefficients, z^{*} denotes the complex conjugate of the complex number z, and $\overline{n} = -n$. For historical reasons, the coefficients

$$W_{lmn} = (-1)^{m-n} \sqrt{\frac{2}{2l+1}}\, c_{mn}^{l}$$

are more commonly used in the literature of materials science. We shall use W_{lmn} below and refer to them also as texture coefficients. For polycrystalline samples, texture coefficients with even l are routinely ascertained by inversion of pole figures obtained from X-ray measurements.

All the texture coefficients vanish when the constituting crystallites of the polycrystal in question have no preferred orientations. In this case,

$$w = w_{\text{iso}} \equiv \frac{1}{8\pi^2}.$$

The polycrystalline aggregate in question may enjoy texture symmetry. For each rotation $\boldsymbol{Q}$ in the group of texture symmetry G_{tex}, we have $w(\boldsymbol{Q}^{\mathrm{T}}\boldsymbol{R}) = w(\boldsymbol{R})$ for each rotation $\boldsymbol{R}$ in G; here $\boldsymbol{Q}^{\mathrm{T}}$ denotes the transpose of $\boldsymbol{Q}$.

THEORETICAL SETTING

We consider sheet metals that have a distinguished rolling direction in the sheet plane, which is a two-fold axis of rotational symmetry of the texture. Henceforth we choose the spatial coordinate system such that the rolling direction (RD), transverse direction (TD), and normal direction (ND) of the sheet agree with the 1-, 2-, and 3-coordinate axis, respectively. In a typical uniaxial tension test, a standard specimen $S(\alpha)$ whose middle axis (in the length direction) makes an angle α with RD is cut from the sample sheet. The specimen is then subjected to uniaxial tension until it is in plastic flow.

Let $f(\sigma, w)$ and $g(\sigma, w)$ be the plastic potential and the yield function of the sheet metal in question; here σ denotes the deviator of the Cauchy stress, and w is the ODF that describes the current texture. Let $\boldsymbol{R}(\boldsymbol{e}_3, \omega)$ be the rotation about $\boldsymbol{e}_3$ by the angle ω, and let $\boldsymbol{s}_1 = \sigma(\boldsymbol{e}_1 \otimes \boldsymbol{e}_1 - \boldsymbol{I}/3)$. The uniaxial flow stress σ satisfies the equation

$$g(\boldsymbol{R}(\boldsymbol{e}_3,\alpha)\boldsymbol{s}_1\boldsymbol{R}(\boldsymbol{e}_3,\alpha)^{\mathrm{T}}, w) = C,$$

where C is a parameter depending on the state of strain hardening. In what follows we report our formulae for the angular dependence of σ and of $q = r/(r+1)$.

FORMULAE FOR ANGULAR DEPENDENCE

By exploiting (i) material frame-indifference, (ii) the intrinsic symmetry in the definition of the q-value and in the uniaxial tension tests considered (namely that σ remains invariant under all rotations about the tension axis, which lies in the plane of the sheet metal), and (iii) the fact that the sheet metals in question have a distinguished rolling direction (which is a two-fold axis of rotational symmetry), we derive general formulae relating the angular dependence of the q-value and of the uniaxial flow stress σ to w, which are valid up to terms linear in the texture coefficients W_{lmn}.

The formulae in question take a simpler form when the polycrystalline aggregate and its constituting crystallites enjoy higher texture and crystal symmetry, respectively. In what follows we present the formulae for the two most important cases in practice:

Orthorhombic Sheets of Cubic Crystallites

$$
\begin{aligned}
q = \frac{1}{2} &+ b_1(\sigma)\left(W_{400} - \frac{2\sqrt{10}}{5} W_{420}\cos 2\alpha - \frac{\sqrt{70}}{5} W_{440}\cos 4\alpha \right) \\
&+ b_2(\sigma)\left(W_{600} - \frac{17\sqrt{105}}{105} W_{620}\cos 2\alpha + \frac{\sqrt{14}}{7} W_{640}\cos 4\alpha + \frac{\sqrt{231}}{7} W_{660}\cos 6\alpha \right) \\
&+ b_3(\sigma)\left(W_{800} - \frac{32\sqrt{35}}{105} W_{820}\cos 2\alpha + \frac{2\sqrt{154}}{21} W_{840}\cos 4\alpha - \frac{\sqrt{1430}}{15} W_{880}\cos 8\alpha \right) \\
&+ \text{terms involving } W_{lmn} \text{ with } l \geq 9,
\end{aligned}
$$

$$
\begin{aligned}
\sigma = \sigma_{\text{iso}} &+ a_1(\sigma_{\text{iso}})\left(W_{400} - \frac{2\sqrt{10}}{3} W_{420}\cos 2\alpha + \frac{\sqrt{70}}{3} W_{440}\cos 4\alpha \right) \\
&+ a_2(\sigma_{\text{iso}})\left(W_{600} - \frac{\sqrt{105}}{5} W_{620}\cos 2\alpha + \frac{3\sqrt{14}}{5} W_{640}\cos 4\alpha - \frac{\sqrt{231}}{5} W_{660}\cos 6\alpha \right) \\
&+ a_3(\sigma_{\text{iso}})\left(W_{800} - \frac{12\sqrt{35}}{35} W_{820}\cos 2\alpha + \frac{6\sqrt{154}}{35} W_{840}\cos 4\alpha - \frac{4\sqrt{429}}{35} W_{860}\cos 6\alpha \right. \\
&\left. + \frac{3\sqrt{1430}}{35} W_{880}\cos 8\alpha \right) + \text{terms involving } W_{lmn} \text{ with even } l \geq 10,
\end{aligned}
$$

where σ_{iso}, the flow stress for the corresponding isotropic sheet, satisfies the equation

$$g(\boldsymbol{R}(\boldsymbol{e}_3,\alpha)\boldsymbol{s}_1\boldsymbol{R}(\boldsymbol{e}_3,\alpha)^{\mathrm{T}}, w_{\text{iso}}) = C.$$

We have obtained terms up to $l = 22$ in the formulae above but refrain from writing them all down for want of space. Readers interested in more details should contact the principal investigator.

Orthorhombic Sheets of Hexagonal Crystallites

$$q = \frac{1}{2} + b_1(\sigma)\left(W_{200} + \frac{\sqrt{6}}{3} W_{220} \cos 2\alpha \right)$$
$$+ b_2(\sigma)\left(W_{400} - \frac{2\sqrt{10}}{5} W_{420} \cos 2\alpha - \frac{\sqrt{70}}{5} W_{440} \cos 4\alpha \right)$$
$$+ b_3(\sigma)\left(W_{600} - \frac{17\sqrt{105}}{105} W_{620} \cos 2\alpha + \frac{\sqrt{14}}{7} W_{640} \cos 4\alpha + \frac{\sqrt{231}}{7} W_{660} \cos 6\alpha \right)$$
$$+ b_4(\sigma)\left(W_{606} - \frac{17\sqrt{105}}{105} W_{626} \cos 2\alpha + \frac{\sqrt{14}}{7} W_{646} \cos 4\alpha + \frac{\sqrt{231}}{7} W_{666} \cos 6\alpha \right)$$
+ terms involving W_{lmn} with $l \geq 7$.

$$\sigma = \sigma_{\text{iso}} + a_1(\sigma_{\text{iso}})\left(W_{200} - \sqrt{6}\, W_{220} \cos 2\alpha \right)$$
$$+ a_2(\sigma_{\text{iso}})\left(W_{400} - \frac{2\sqrt{10}}{3} W_{420} \cos 2\alpha + \frac{\sqrt{70}}{3} W_{440} \cos 4\alpha \right)$$
$$+ a_3(\sigma_{\text{iso}})\left(W_{600} - \frac{\sqrt{105}}{5} W_{620} \cos 2\alpha + \frac{3\sqrt{14}}{5} W_{640} \cos 4\alpha - \frac{\sqrt{231}}{5} W_{660} \cos 6\alpha \right)$$
$$+ a_4(\sigma_{\text{iso}})\left(W_{606} - \frac{\sqrt{105}}{5} W_{626} \cos 2\alpha + \frac{3\sqrt{14}}{5} W_{646} \cos 4\alpha - \frac{\sqrt{231}}{5} W_{666} \cos 6\alpha \right)$$
+ terms involving W_{lmn} with even $l \geq 8$.

Again, readers interested to see more terms in the two formulae above should contact the principal investigator.

EXPERIMENTAL INVESTIGATIONS ON AN ALUMINUM ALLOY

The formulae given above will not be useful in practice unless we may truncate them at a relatively small l for a particular material in question. For instance, past experience has indicated that for cold-rolled steel sheets we may truncate the formulae above for cubic metals at $l = 4$, but doing so will be inadequate for aluminum. At the University of Kentucky we conducted measurements on a commercial AA5xxx hot band and its O-temper counterpart to check the adequacy of the above formulae when they are truncated at $l = 6$:

$$q = \frac{1}{2} + b_1(\sigma)\left(W_{400} - \frac{2\sqrt{10}}{5} W_{420}\cos 2\alpha - \frac{\sqrt{70}}{5} W_{440}\cos 4\alpha \right) + b_2(\sigma)\left(W_{600} - \frac{17\sqrt{105}}{\cdot 105} W_{620}\cos 2\alpha + \frac{\sqrt{14}}{7} W_{640}\cos 4\alpha + \frac{\sqrt{231}}{7} W_{660}\cos 6\alpha \right) \quad (3)$$

$$\sigma = \sigma_{iso} + a_1(\sigma_{iso})\left(W_{400} - \frac{2\sqrt{10}}{3} W_{420}\cos 2\alpha + \frac{\sqrt{70}}{3} W_{440}\cos 4\alpha \right) + a_2(\sigma_{iso})\left(W_{600} - \frac{\sqrt{105}}{5} W_{620}\cos 2\alpha + \frac{3\sqrt{14}}{5} W_{640}\cos 4\alpha - \frac{\sqrt{231}}{5} W_{660}\cos 6\alpha \right) \quad (4)$$

here σ_{iso}, the flow stress for the corresponding isotropic sheet, may change with strain hardening.

The textures of the two mother sheets (AA5xxx hot band and O-temper) were measured by X-ray diffraction. The relevant texture coefficients are reported in Table 1. For each angle θ of 0°, 15°, 30°, 45°, 60°, 75°, and 90°, two uniaxial tension test specimens were cut from each mother sheet. Uniaxial tension tests were conducted on these 28 specimens. In each test the specimen was pulled beyond yield to a certain strain and then completely unloaded. The natural longitudinal strain ε_l and transverse strain ε_t after the unloading were recorded, and the highest uniaxial stress σ before the unloading was taken as the flow stress corresponding to these plastic strains.

The test specimen was subsequently reloaded beyond yield to a higher strain and then completely unloaded. The loading and unloading cycle was repeated until ε_l reached about 5% for the hot band and about 10% for the O-temper specimens. For each specimen, the q-value was found to be constant over the range of ε_l in question, whereas σ increased with ε_l. As shown in Fig. 1, by taking $b_1 = -9.2$, $b_2 = 11.3$ for the hot band and $b_1 = -20.9$, $b_2 = 4.7$ for the O-temper sheet, Eq. (3) fits the experimental data on the q-value rather well. The same can be said of Eq. (4) and the flow stress σ, where the fittings in Fig. 2 pertain to $\sigma_{iso} = 266$ MPa, $a_1 = -367$ MPa, $a_2 = -529$ MPa for the hot band, and $\sigma_{iso} = 156$ MPa, $a_1 = 971$ MPa, $a_2 = 263$ MPa for the O-temper sheet.

Table 1: Texture Coefficients of AA5xxx Hot Band and O-Temper Samples

	W_{400}	W_{420}	W_{440}	W_{600}	W_{620}	W_{640}	W_{660}
HB	−0.0033	−0.0025	−0.0071	−0.0048	0.0062	−0.0032	−0.0011
O	0.0072	−0.0019	0.0022	0.0004	0.0007	−0.0017	0.0004

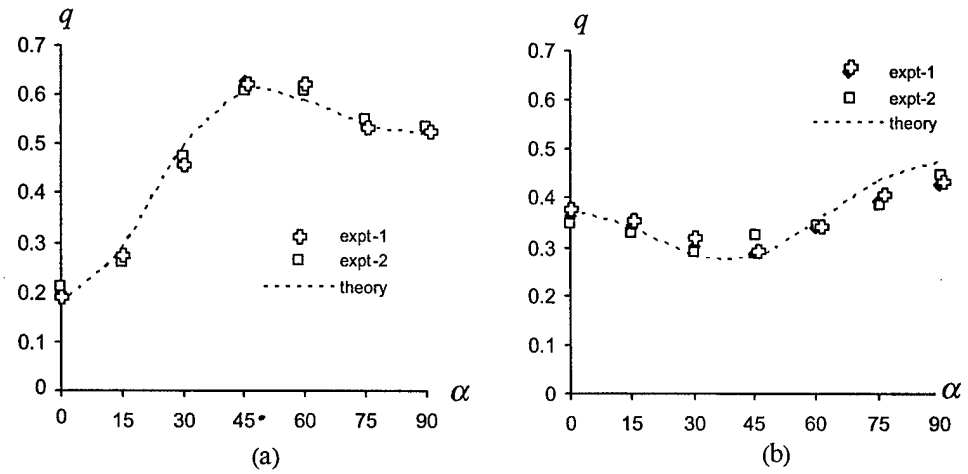

Figure 1. Plots of angular dependence of the q-value of an AA5xxx aluminum alloy: (a) hot band; (b) O-temper sheet.

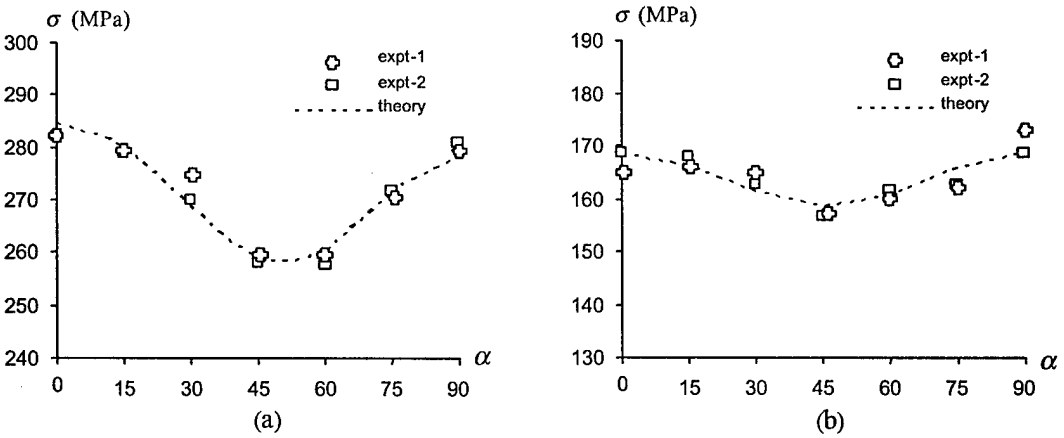

Figure 2. Plots of angular dependence of the uniaxial flow stress at 4% plastic longitudinal strain for an AA5xxx aluminum alloy: (a) hot band; (b) O-temper sheet.

Equations (3) and (4), with specific b_i and a_i, follow (cf. journal paper [6]) from a cubic plastic potential f and yield function g proposed by Man. Our analysis of the measurement data indicates that, at least for this cubic form of plastic potential and yield function, $f \neq g$ both for the AA5xxx hot band and for its O-temper counterpart.

In summary, Eqs. (3) and (4) were found to be adequate for describing the angular dependence of the q-value and the flow stress anisotropy of the AA5xxx alloy sheets in question. The annealing treatment, which made an O-temper sheet out of the hot band, drastically changed not only the crystallographic texture of the hot band, but also the values of the parameters b_i, a_i, and σ_{iso} in Eqs. (3) and (4). While it is a common assumption in the literature of metal plasticity that the yield function serves also as the plastic potential, our study suggests that this assumption may not be valid for the strip-cast AA5xxx aluminum alloy in question, which is an interesting problem that merits further investigation.

Contributions to Acoustoelasticity

The velocities of ultrasonic waves propagating in a material body are affected by the stress present. This phenomenon is called the acoustoelastic effect. Conversely, the possibility of using this effect as a means for nondestructive evaluation of stress gives the impetus for the study of acoustoelasticity.

During the course of this project, we made several contributions to acoustoelasticity, among which we single out the following two as the most significant:

- A constitutive relation pertaining to acoustoelasticity was formulated for prestressed, orthorhombic aggregates of cubic crystallites. This constitutive relation accounts for the effects of crystallographic texture explicitly and will serve as the basis for all further work in acoustoelasticity for the class of polycrystalline materials in question. Cf. journal paper [2] listed in the Executive Summary.
- For vertically-heterogeneous, prestressed orthorhombic media where the principal stress directions agree with the axes of orthorhombic material symmetry, a high-frequency asymptotic formula was derived which relate the depth variations of stress and texture to the dispersion of surface acoustic waves propagating in a symmetry direction. Here the elastic medium in question is taken as occupying a half-space. This theory and its further developments have an important potential application in the nondestructive inspection of the thin layer of inhomogeneous stress induced by surface enhancement techniques such as shot peening, laser shock peening, and low plasticity burnishing. Cf. conference papers [5], [8] and [13] listed in the Executive Summary.